Check for updates

ADVANCED THERAPEUTICS
www.advtherap.com

An Adaptable Antibody-Based Platform for Flexible Synthetic Peptide Delivery Built on Agonistic CD40 Antibodies

Mohamed Eltahir, Ida Laurén, Martin Lord, Aikaterini Chourlia, Leif Dahllund, Anders Olsson, Aljona Saleh, A. Jimmy Ytterberg, Annika Lindqvist, Oskar Andersson, Helena Persson, and Sara M. Mangsbo**

The agonistic potentials of therapeutic anti-CD40 antibodies have been profiled in relation to antibody isotype and epitope specificity. Still, clinical impact relies on a well-balanced clinical efficacy versus target-mediated toxicity. As CD40-mediated immune activation must rely on a combination of stimulation of antigen-presenting cells (APCs) alongside antigen presentation, for efficient T cell priming, alternative approaches to improve the therapeutic outcome of CD40-targeting strategies should focus on providing optimal antigen presentation together with CD40 stimulation. Herein, a bispecific antibody targeting CD40 as a means to deliver cargo (i.e., synthetic peptides) into APCs through a non-covalent, high-affinity interaction between the antibody and the cargo peptide, further referred to as the Adaptable Drug Affinity Conjugate (ADAC) technology, has been developed. The ADAC platform demonstrated a target-specific $CD4^+$ and $CD8^+$ T cell expansion in vitro and significantly improved peptide-specific $CD8^+$ T cell proliferation in vivo. In addition, the strategy dramatically improved the in vitro and in vivo half-life of the synthetic peptides. Future applications of ADAC involve pandemic preparedness to viral genetic drift as well as neoepitope vaccination strategies where the bispecific antibody is an off-the-shelf product, and the peptide antigen is synthesized based on next-generation sequencing data mining.

1. Introduction

Antigen delivery in the form of synthetic peptide-based vaccines has commonly been performed using lipid or nanoparticle-based technologies with and without the addition of adjuvants.[1,2] Depot delivery of peptide-based drugs using these formulations can prevent rapid degradation and drug clearance, but trimmed peptides (HLA-matched epitopes) delivered in a lipid-based formulation have also been reported to trap expanded antigen-specific cells.[3] Vector-based antigen delivery can lead to antigen competition of potent viral epitopes, thereby hampering anti-tumor responses, which may be tackled using a shift in vector between the prime and the boost delivery time-point.[4] Antibody-based delivery platforms can be utilized by conjugating proteins or peptides, forming antibody-drug conjugates where the antigen is the cargo. This approach has been studied using several dendritic cell (DC) protein targets such as c-type lectins (e.g., DEC-205, Dectin-1, CD207, LOX-1, and others) and non-lectins like mannose receptors, integrins, and CD40.[5]

However, not all targets and antibodies facilitate both activation of the DC along with enabling antigen uptake. Furthermore, it is important that the receptor-mediated internalization should not lead to a loss of antigen on the surface, but rather a recycling of the targeted antigen, and possibly an increased expression over time as activation takes place. Targeting the CD40 receptor on DCs for antigen delivery via coupling of the antigen to an

M. Eltahir, I. Laurén, M. Lord, A. Chourlia, S. M. Mangsbo
Department of Pharmacy
Science for Life Laboratory
Uppsala University
Husargatan 3, Uppsala Box 580 751 24, Sweden
E-mail: mohamed.eltahir@igp.uu.se; sara.mangsbo@farmaci.uu.se

The ORCID identification number(s) for the author(s) of this article can be found under https://doi.org/10.1002/adtp.202200008

© 2022 The Authors. Advanced Therapeutics published by Wiley-VCH GmbH. This is an open access article under the terms of the Creative Commons Attribution License, which permits use, distribution and reproduction in any medium, provided the original work is properly cited.

DOI: 10.1002/adtp.202200008

L. Dahllund, A. Olsson, O. Andersson, H. Persson
SciLifeLab Drug Discovery and Development
Science for Life Laboratory – Stockholm
Tomtebodavägen 23A, Solna 171 65, Sweden

L. Dahllund, A. Olsson, O. Andersson, H. Persson
School of Engineering Sciences in Chemistry
Biotechnology and Health
Royal Institute of Technology (KTH)
Tomtebodavägen 23A, Solna 65, Sweden

A. Saleh, A. J. Ytterberg, A. Lindqvist
Department of Pharmacy
SciLifeLab Drug Discovery and Development Platform
Uppsala University
Husargatan 3, Uppsala Box 580 751 24, Sweden

anti-CD40 antibody has been shown to elicit superior $CD8^+$ cross-priming and a CD8-specific immune memory response.[5–8] Besides this, the use of anti-CD40 antibody conjugates also results in the achievement of robust adjuvant response at a lower dose, which is vital in limiting the toxic effects of systemic anti-CD40 therapy.[6]

Each tumor is unique, and there is a growing interest in neoantigen vaccination. However, individualized peptide-based vaccines are challenging to produce, formulate, and deliver.[9] Herein we have built a protein-based platform, in the form of a bispecific tetravalent antibody, for optimized targeting, activation of DCs and improved antigen uptake. The platform uses an affinity-based approach, further named the Adaptable Drug Affinity Conjugate (ADAC) technology, where the cargo peptide antigen is non-covalently linked to an agonistic anti-CD40 antibody. The high-affinity interaction, accomplished via a second binding domain through a peptide-Tag (pTag), ensures the binding of the cargo antigen to the antibody and its release within the cell.

Several strategies have been investigated to deliver the agonistic CD40 signal to the DCs where the tumor antigens are present to ensure the appropriate adjuvant effect of agonistic anti-CD40 antibodies. These include administering anti-CD40 antibodies intratumorally, where tumor antigen shedding ensures antigen and antibody lymph node drainage, leading to antigen presentation and immune stimulation at the same site.[10–12] Besides posing superior efficiency over systemic administration, this approach reduces adverse effects.[12] However, it may lead to the expansion of tumor-associated myeloid-derived suppressor cells.[13] Another approach involves the covalent coupling of the tumor antigen to an anti-CD40 antibody. This conjugation approach has been tested experimentally with several antigens, including herpes simplex glycoprotein,[6] an influenza peptide split virus or whole virus vaccines,[7] and with the A20 lymphoma idiotype.[8] This approach has shown better immunogenicity and superior efficiency at a lower dose of vaccination than non-linked antigen material mixed with the antibody.

However, conjugating the tumor antigens to the anti-CD40 antibody is a laborious and challenging process, and the final product is rigid and unadaptable due to the nature of the chemical conjugation. ADAC is a flexible platform for antigen-adjuvant delivery to the relevant antigen-presenting cells (APCs) through CD40. This approach enables the antibody development as an adjuvant product, whereas the peptide synthesis and release through regulatory process approval is a separate entity rather than a specific drug market approval. By avoiding the need for complex chemical conjugation, the ADAC platform provides a versatile approach for varying the tumor antigen, thereby facilitating the personalization of cancer patient therapy and offering a feasible way to manage vaccine adaptation with viral genetic drift in a pandemic situation.

2. Experimental Section

2.1. In Vitro and In Vivo Materials and Reagents

B3Z, pmel-1, or OT-II cells were used for the T cell proliferation and activation assays. B3Z is a T cell hybridoma expression T cell receptor (TCR) that recognizes MHC-I loaded with $OVA_{257\text{-}264}$ albumin peptide (SIINFEKL). B3Z cells express β-galactosidase under the interleukin (IL)-2 promoter, converting chlorophenol Red-β-D-galactopyranoside (CPRG) substrate and enabling detection of B3Z activation via absorbance readout.[14] The pmel-1 transgenic strain expresses the TCR specific for MHC-I/$hgp100_{25\text{-}33}$ (KVPRNQDWL).[15] The OT-II transgenic strain consists of T cells expressing the TCR specific for the MHC-II/peptide $OVA_{323\text{-}339}$ (ISQAVHAAHAEINEAGR).[16] $CD8^+$ T cells from pmel-1 or $CD4^+$ T cells from OT-II splenocytes were isolated by harvesting spleens and inguinal lymph nodes from adult B6. Cg-Thy1a/Cy Tg (TcraTcrb)8Rest/J transgenic mice (pmel-1 mice) or C57BL/6-Tg-(TcraTcrb)425Cbn/Crl transgenic mice, (OT-II mice), respectively (The Jackson Laboratory). The organs were carefully mashed and passed through 70 μm cell strainers to achieve single-cell suspensions, and red blood cells were lysed using RBC lysis buffer (eBioscience). For in vitro experiments, pmel-1 $CD8^+$ cytotoxic T cells were isolated using Dynabeads Untouched Mouse CD8 Cells Kit, and the OT-II $CD4^+$ helper T cells were isolated using Dynabeads Untouched Mouse CD4 Cells Kit (both from Invitrogen). Long bones from transgenic human CD40 mice were kindly provided by Dr. Peter Ellmark (Alligator Biosciences, Lund, Sweden). Bone marrow progenitor cells were isolated from the long bones and differentiated to bone marrow-derived dendritic cells (BMDC) (described below). For in vivo experiments, pmel-1 and OT-II mice (The Jackson Laboratory) were bred and housed in the Uppsala Biomedical Center's (BMC) animal facility. For in vivo experiments, all animals were between 8–15 weeks of age at the time of the experiment. Both female and male mice were used in the in vivo experiments. For a given single experiment, one gender, female or male mice, we used.

2.2. Antibody Constructs

The tetravalent bispecific antibodies used in these studies are composed of an anti-CD40 monoclonal antibody and a tag moiety binding part. The two anti-CD40 antibodies used were CP-870.893 or 1150/1151 (further on named 1150), described in WO 2015/09 1853. Genes encoding the variable parts of the heavy chain, VH, and light chain, VL, were kindly provided by Dr. Peter Ellmark (Alligator Biosciences, Lund, Sweden). The VH and VL regions were PCR amplified and inserted into modified versions of the pIgG vector (GenBank: MK988448.1), using the In-Fusion HD Plus Cloning Kit (Clontech, #638 909). Two antibodies of each clone were constructed, differing in IgG subclass, IgG1 or IgG2. CP-870893 of the IgG1 and IgG2 subclasses were named CP-1 and CP-2, respectively. Analogously, the two subclass variants of the 1150 antibody were denoted 1150–1 and 1150–2 (**Table 1**). Based on these parental constructs, tetravalent bispecific antibodies, named Bispecific/Tagged-peptide antibody (BiTag), were constructed through fusion with one of two different anti-Tag single-chain variable fragments (scFv); 14GIIICII or FITC8. 14GIIICII originates in a mouse IgG1 antibody, previously generated by immunization of mice with a linear B-cell epitope of tetanus toxin (amino acid sequence FIGITELKKLESKINKVF).[17] Hybridoma sequencing, outsourced to Absolute Antibody (Redcar, United Kingdom), was performed by proprietary next-generation sequencing (NGS)-based technology. The VH and VL

© 2022 The Authors. Advanced Therapeutics published by Wiley-VCH GmbH

Table 1. List of parental and BiTag antibodies used in the different in vitro and in vivo models.

Antibody	Isotype of anti-CD40	Anti-CD40 antibody	scFv	Location of scFv	Bispecific
Bi1-CP	h-IgG1	CP-870.893	Anti-pTag	CH3	Yes
Bi2-CP	h-IgG2	CP-870.893	Anti-pTag	CH3	Yes
Bi3-CP	h-IgG1	CP-870.893	Anti-pTag	CL	Yes
Bi9-1150	h-IgG1	1150	Anti-pTag	CH3	Yes
Bi10-1150	h-IgG2	1150	Anti-pTag	CH3	Yes
Bi11-1150	h-IgG1	1150	Anti-pTag	CL	Yes
Bi17-CP	h-IgG2	CP-870.893	Anti-fTag	CH3	Yes
CP-1	h-IgG1	CP-870.893	–	–	No
CP-2	h-IgG2	CP-870.893	–	–	No
1150-1	h-IgG1	1150	–	–	No
1150-2	h-IgG2	1150	–	–	No

regions were successfully assembled and sequenced, and based on these, a gene encoding an scFv was formed by fusing the VH to the VL, N-terminal to C-terminal, via a glycine-serine linker ((Gly4Ser)4). Protein expression and subsequent surface plasmon resonance (SPR) experiments suggested that the scFv fully retained the antigen-binding ability of its full-length parental IgG counterpart (data not shown). PCR amplification and In-Fusion cloning was subsequently used to fuse the 14GIIICII scFv gene to the four anti-CD40 vector constructs, either to the C-terminal end of a heavy (CH3) or light chain (CL) through a (Gly4Ser)2 linker. Altogether, this procedure gave rise to six BiTag constructs. An overview of these is shown in Table 1, and a schematic representation is depicted in **Figure 1**. The final expression vectors were transformed into Escherichia coli cells and plasmid DNA isolated, and their intended designs were confirmed by DNA sequencing. In addition, a seventh BiTag antibody was constructed, named Bi17-CP. This BiTag is composed of the human anti-fluorescein scFv FITC8 (GeneBank, accession number AX814386.1) fused to the CH3 of CP-2 (Table 1). FITC8 was generated by phage display and bind fluorescein (in the context of this work, denoted fluorescent Tag [fTag]) with an affinity of ≈0.9 nM.[18] Cloning of this construct was outsourced to Absolute Antibody, using the same linker regions as described above.

2.3. Antibody Expression, Purification, and Biophysical Analyses

Parental and BiTag antibodies were expressed by transient transfection of human embryonic kidney cells in suspension. Transfection of plasmid DNA into ExpiHEK293FTM cells (ThermoFisher, #A14527) was performed using an ExpiFectamine 293 Transfection Kit (ThermoFisher, #A14525). After six days of cultivation at 37 °C, 8% CO2, 70% rH, and 125 rpm, the media supernatants were purified in two steps by affinity chromatography using a HiTrap Protein A HP column (Cytiva) and HiLoad 16/600 Superdex 200 size exclusion chromatography (SEC) (Cytiva) on an ÄKTA purifier system. The size exclusion pools were concentrated to a volume of ≈1 mL or a concentration of at least 1 mg mL^{-1} by Pierce Protein Concentrators (PES, 5–20 mL) with a molecular cut-off of 30 kDa (Thermo Scientific, #88 531). The

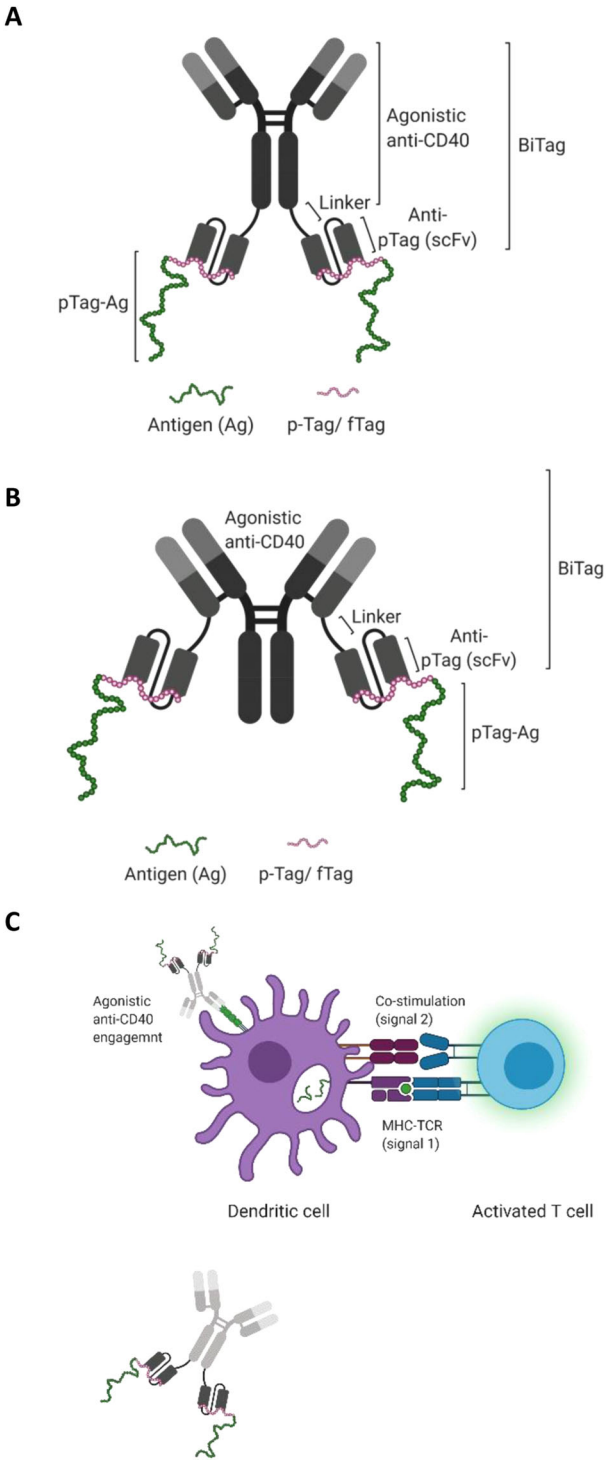

Figure 1. Illustration of the ADAC platform and target binding. Schematic representation of the design of the BiTag. A tetravalent bispecific antibody consists of an agonistic anti-CD40 hIgG1 or hIgG2 antibody covalently linked to two identical scFv targeting a linear pTag on the C-terminal of A) CH3 or B) CL. The peptide antigen is a synthetic long peptide with a constant pTag or fTag and a variable tumor antigen (Ag). C) The BiTag platform enables simultaneous delivery of antigen (signal 1) and co-stimulation to the T cells (signal 2), resulting in robust T cell activation. Illustrations are created with BioRender.com.

© 2022 The Authors. Advanced Therapeutics published by Wiley-VCH GmbH

Table 2. List of peptide antigens (pTag-Ag) used for the different in vitro and in vivo models. Underlined: pTag sequence, Bold: T cell epitope (Ag).

Peptide	Peptide identity	Sequence
UU05	**pTag-SIINFEKL (long)**	FIGITELKKLESKINKVFLEQLE**SIINFEKL**AAAAAK
UU10	SIINFEKL (long)	LEQLE**SIINFEKL**AAAAAK
UU23	**pTag-SIINFEKL(short)**	FIGITELKKLESKINKVF**SIINFEKL**
UU24	**pTag-Biotin**	FIGITELKKLESKINKVF-Biotin
UU25	**pTag-OVA (protein)**	FIGITELKKLESKINKVF-OVA (protein)
UU30	**pTag-** gp100$_{25\text{-}33}$ **(long)**	FIGITELKKLESKINKVFAVGAL**KVPRNQDWL**GVPRQL
UU33	gp100$_{25\text{-}33}$ **(short)**	**KVPRNQDWL**
UU44	**fTag-** CMV pp65$_{495\text{-}503}$ **(long)**	FITC(Ahx)AGILAR**NLVPMVATV**QGQNLKY
UU60	**pTag-** OT-II$_{323\text{-}339}$ (long)	FIGITELKKLESKINKVFISQAVH**AAHAEINEA**GR

protein concentration of the purified proteins was determined by measuring absorbance at 280 nm. Purity and integrity of the antibodies were assessed by SDS-PAGE, and monomeric content was determined by analytical SEC performed using a Bio SEC-3 column (300A, 7.8 × 300 mm) (Agilent), connected to an Agilent 1260 Infinity system and using 0.15 M Na*x*HyPO4 pH 6.8 at a flow rate of 1 mL min^{-1}. Endotoxin levels were determined using an Endosafe PTS instrument (Charles River) and cartridges with a minimum detection limit of 0.05 EU/mL.

The particle size distribution of the purified antibodies was analyzed by dynamic light scattering (DLS) using a Zetasizer Ultra (Malvern Panalytical). Antibody aggregation was assessed by analytical SEC, as described above, after one freeze–thaw cycle at −80 °C. Subsequently, the purified proteins were aliquoted and stored at −80 °C. Antibody expression and purification of Bi17-CP were outsourced to Absolute Antibody, using a similar procedure as just described. In short, HEK293 cells were used as expression hosts, purification performed by protein A affinity purification followed by preparative SEC and quality assessed by SDS-PAGE, analytical SEC, and measurements of endotoxin levels. All antibody constructs stocks had endotoxin level <1 EU/mL and final endotoxin levels in cultures were never above 0.03 EU/mL.

2.4. Tagged Antigenic Peptides (pTag-Ag)

Synthetic long peptides (SLPs) were custom purchased from Capra Science (Sweden) or TAG Copenhagen (Denmark). **Table 2** describes the amino acid sequence of the SLPs used.

2.5. Characterization of Antigen Binding

Parental and BiTag antibodies were assayed for CD40 binding and either of the two tag moieties, pTag or fTag. Biotinylated antigens were immobilized into the wells of a 384 ELISA plate via streptavidin (2 µg mL^{-1}) at a concentration of 0.1 µg mL^{-1} for human CD40 (Acro-Biosystems, #CD0-H82E8) and the model pTag (FIGITELKKLESKINKVF-biotin, Capra Biosciences, Lund, Sweden), named UU24 (Table 2), in PBT (PBS + 0.5% bovine serum albumin [BSA] + 0.05% Tween20). In the case of Bi17-CP, binding to a fluorescein isothiocyanate (FITC)-labeled mouse antibody was assessed to confirm the binding of the anti-fTag scFv. After each incubation step, plates were washed 3–4 times with PBS supplemented with 0.05% Tween20. The purified antibodies, diluted to 0.2 µg mL^{-1}, were added to the wells. Detection of binding was performed using horseradish peroxidase (HRP)-labeled anti-human IgG kappa antibody (Southern Biotech), followed by incubation with the chromogen Ultra TMB-ELISA (Thermo-Scientific Pierce). Signal development was stopped by adding 1 M sulfuric acid, and the absorbance was measured at 450 nm.

Simultaneous binding of the two antigen-binding sites was assessed by ELISA and SPR-based approach. In ELISA, an Fc-fused CD40 protein (RnD Systems, #1493-CDB) was immobilized in the wells, the purified antibodies added, followed by the addition of biotinylated peptides; UU24 or a scrambled peptide (EKLINKLSKIFKGTIE). The binding was detected by HRP-labeled streptavidin (Sigma-Aldrich), and development was performed as above. In the SPR experiments, a Biacore T200 instrument (Cytiva) was used. The biotinylated pTag UU24 was captured onto a streptavidin-coated SPR biosensor chip (Cytiva). BiTag antibodies were injected, diluted to reach a response level between 200 and 300 RU, followed by the injection of 50 nM CD40-Fc (RnD Systems, #1493-CDB). The surfaces were regenerated with 10 mM glycine-HCl, pH 2.1. The running buffer used was HBS-EP+ (0.01 M HEPES, pH 7.4, 0.15 M NaCl, 3 mM EDTA, 0.05% [v/v] Tween 20), and all samples were diluted in this buffer before injection.

Affinity and kinetic constants of the parental and BiTag antibodies were assessed using single cycle kinetics (SCK) SPR approach. An anti-human Fab antibody (Cytiva, #28 958 325), functioning as a capture ligand, was immobilized through EDC/NHS chemistry onto all four surfaces of a CM5-S amine sensor chip according to the manufacturer's recommendations. Antibodies were injected and captured onto the chip surface. Three channels were used to capture different antibodies, whereas channel 1 was used as a reference surface. Threefold dilution series of five concentrations of the two human CD40 versions; the monomeric avi-tagged version (AcroBiosystems, #CD0-H82E8) and the dimeric Fc-fused variant (RnD Systems, #1493-CDB), were prepared in HBS-EP+ buffer and sequentially injected over the chip surfaces. More specifically, a concentration range of 12–1000 nM CD40-avi and 0.6–50 nM CD40-Fc were used to analyze the 1150-based parental and BiTag constructs. The corresponding ranges for the CP-870893-based antibodies were 1.2–100 and 0.6–50 nM. Following a dissociation phase of 600 to 1200

© 2022 The Authors. Advanced Therapeutics published by Wiley-VCH GmbH

s, the surfaces were regenerated with 10 mM glycine-HCl (pH 2.1). Response curve sensorgrams were obtained after removing the reference channel's response and a reference cycle (running buffer instead of antigen). Reaction rate kinetics constants were calculated using the Biacore T200 evaluation software 3.1 using the 1:1 Langmuir binding model for all interactions except for 1150-based constructs together with CD40-avi. Here, the steady state binding model was found more feasible and it was used to get an estimation of the affinity (dissociation constant, K_D).

Similarly, the affinity to the pTag was measured using a capture-based SPR-approach. The 14GIIICII scFv was captured through an immobilized anti-FLAG antibody, and measurement was performed as previously described by Preger et al.[19] The corresponding binding of the BiTag antibodies was performed using capture through the anti-Fab antibody as described above. The pTag-Ag, UU30, was injected in threefold dilution series of five concentrations ranging between 0.62–50 nM, and reaction rate kinetics were calculated using the 1:1 Langmuir binding model as described.

2.6. Analysis of Binding to Fc gamma Receptors (FcγR) and Neonatal Fc Receptor (FcRn)

Binding to a panel of different Fc receptors was also measured by SPR using a Biacore T200 instrument of the four parental antibodies and all the BiTag antibodies except for Bi17-CP. Biotinylated CD40 (AcroBiosystems, #CD0-H82E8) was captured onto a streptavidin-coated SPR biosensor chip (Cytiva) to a response unit (RU) level ≈2000. The different antibodies were injected, aiming for RU levels of ≈240 and ≈320 for parental and BiTag antibodies, respectively. This step was followed by injection of 100 nM of the various human recombinant produced Fc receptors (R&D systems); FcRn (#8639-FC-050), FcγRIIIA, (#4325-FC-050), FcγRIIIB (#1597-FC-050/CF), and FcγRIIA(#1330-CD-050). For FcRn, a lower pH phosphate buffer (100 mM NaPO4, 150 mM NaCl, 0.05% Tween20, at pH 6.0) was used as a running and dilutant buffer, whereas HBS-EP+ (pH 7.4) was used for the other receptors. The surfaces were regenerated using 10 mM glycine-HCl (pH 2.1). The obtained sensorgrams were visually inspected, and the binding response of the bispecific antibodies was compared to the matching parental IgG, taking into account differences in antibody capture levels and molecular weights.

2.7. LC-MS/MS

All pTag peptides and tryptic antibody peptides from Bi10-1150 and 1150–2 were quantified using a TQ-S micro triple quadrupole mass spectrometer connected to an Acquity UHPLC system (Waters Corp). For the pTag peptides UU05, UU23, and UU30, the chromatographic separation was carried out using a BEH C8 column (1.7 μM, 2.1 × 50 mm) with a linear gradient from 0% to 100% mobile phase B within 1.6 min. A reversed-phase Acquity Peptide CSH C18 column (1.7 μm, 2.1 mm × 100 mm) was used for the tryptic antibody peptides, eluted using the following gradient: 0.0–1.0 min, 2% B; 1.10 min, 10% B; 3.1 min, 30% B; 3.6–4.1 min, 100%; B 4.2–6.0 min, 2% B. Mobile phases used consisted of: A) 0.1% formic acid in milliQ H2O and B) 0.1% formic acid in acetonitrile (ACN), and the flow rate was set to 0.5 mL min^{-1}.

All analytes were positively ionized in electrospray (ESI) and monitored in multiple reaction monitoring (MRM) mode with following transitions, collision energy (CE) and cone voltage (Cone): 718.8 > 810.3 (CE: 18 eV, Cone: 15 V) and 616.2 > 740.1 (CE: 12e V, Cone: 10 V) for UU30, 611.2 > 698.5 (CE: 16 eV, Cone: 35 V) and 763.8 > 698.5 (CE: 16 eV, Cone: 35 V) for UU23, 830.5 > 929.8 (CE: 25 eV, Cone: 25 V) and 830.5 > 972.4 (CE: 25 eV, Cone: 15 V) for UU05, 412.8 > 327.1 (CE: 10 eV, Cone 23 V) for GLPAPIEK 2+ (surrogate peptide for quantification of Bi10-1150 and 1150–2), and 423.9 > 662.7 (CE 10 eV, Cone: 23 V) for ALPAPIE[K]2+ (internal standard). The source parameters were set to 0.8 or 2.5 kV for capillary voltage for pTag peptides and tryptic antibody peptides, respectively, 150 °C for source temperature, 650 °C for desolvation gas temperature and 1200 L h^{-1} for desolvation gas flow.

2.8. In Vitro Peptide Stability Assay

UU05, UU23, or UU30 (1–10 μM) were incubated in mouse plasma (K2EDTA anticoagulant, Innovative Research LC), human plasma (sodium citrate anticoagulant, Uppsala University Hospital), or in PBS buffer (pH 7.5) with 2% BSA at 37 °C. The peptides were incubated alone, with the parental antibody 1150–1, or with the BiTag antibody Bi9-1150, at a molar ratio of 1:1 to 1:2 (antibody:peptide), for a duration between 4–24 h. The reaction was stopped at designated time points by adding three volumes of ice-cold methanol. The samples were vortexed and centrifuged for 20 min at 3220 × g at 4 °C, followed by evaporation of supernatant and subsequent reconstitution of dried material in (100 μL) of 2% ACN and 0.5% formic acid in water prior to analysis with LC-MS/MS.

2.9. In Vivo Peptide Stability Assay

C57BL/6 mice were injected using hock injection with the pTag-peptide UU30 +Bi10-1150 or UU30 + 1150–2. Each mouse received the same antibody dose of 2 mg kg^{-1} body weight. The peptide UU30 was co-injected at a molar ratio of 1:2 of antibody to the peptide. Plasma samples along with the draining popliteal and the draining inguinal lymph nodes were collected from the mice at the 0.5, 1.5, 4, and 8-hour time points, and the samples were analyzed for the presence of antibody and intact pTag-peptide. For sample preparation, lymph nodes were weighed individually (Micro balance, Sartorius micro M3P) and homogenized using Ultrasonic processors (Vibra-Cell VCX 130 with 3 mm microtip, SONICS). To each lymph node (popliteal; 0.35 to 3.8 mg, inguinal; 0.43–6.9 mg) 50 μL of 6.4 M urea in 0.1 M ammonium carbonate (ABC) buffer were added before processing. The total protein concentration of the lymph node preparation was measured with the tryptophan fluorescence method.[20] For the quantification of UU30 in the study samples, plasma or lymph node homogenate samples (20 μL) were precipitated with 80 μL methanol. After centrifugation for 20 min (13 000 RPM, MiniSpin Plus, Eppendorf), 85 μL were transferred to glass vials and evaporated (Genevac

© 2022 The Authors. Advanced Therapeutics published by Wiley-VCH GmbH

EZ-2) before resuspension in 70 µL 5% ACN and 0.5% formic acid in water. Bi10-1150 and 1150–2 were quantified by tryptic digestion, SPE for sample concentration and clean up, followed by LC-MS/MS analysis using a signature peptide (GLPAPIEK, 2+) together with an isotopically labeled analog of the signature peptide as the internal standard. Fifteen (15 µL) microliters of plasma was diluted with 37 µL urea (9 M) in 100 mM ABC buffer on a LoBind 96-well plate (Greiner Bio-One 96-Well Conical Bottom) and denatured at ambient temperature for 20 min in a plate shaker at 440 rpm. Alternatively, 15 µL of lymph node homogenate already in 6.4 M urea were added to the plate. Five (5 µL) microliter of dithiothreitol were added (5 mM final concentration) to reduce denatured samples for 40 min at 350 rpm, followed by alkylation with 5 µL of iodoacetamide (10 mM final concentration) at ambient temperature. Unreacted iodoacetamide was quenched with 5 µL of dithiothreitol for 30 min. After dilution with 0.1 M ABC (pH 7.8, final urea concentration 1 M), trypsin was added to an enzyme:substrate (E:S) ratio of 1:20 for the plasma samples, and a median E:S ratio of 1:27 for the lymph node samples (90% of samples between 1:7–1:65). Samples were incubated at 37 °C overnight under agitation at 600 rpm. The reaction was stopped by adding 10% trifluoroacetic acid (2% final concentration), followed by centrifugation for 5 min at 4 °C and 805 × g. The digested samples were purified and concentrated using ProteinWorks μElution SPE Clean-up Kit: MCX (Mixed-Mode Cation-eXchange; Waters). The eluates were then diluted with 50 of µL 5% formic acid in water with stabile isotype labeled internal standard ALPAPIE[K] ($^{13}C_6$, $^{15}N_2$). A volume of 7.5 µL of sample aliquots was injected into LC-MS/MS system.

2.10. Bone Marrow Cell Isolation and BMDC Differentiation

Bone marrow precursor cells from femora and tibiae of adult transgenic human CD40-expressing mice (tghCD40) or wild type (WT) C57BL/6 mice were isolated under sterile conditions. After removing the soft tissue, the bones were disinfected with 70% ethanol before the bone marrow was cut-opened at the bone epiphyses. Bone marrow cells were flushed using IMDM until the bone core became white. Cell clumps were passed through a 70 µm cell strainer to form a single-cell suspension. The cells were washed by centrifugation before they were frozen in 10% DMSO FBS at −160 °C until the time of usage. For BMDC differentiation, bone marrow precursor cells were thawed and cultured for eight days in non-TCT plates at a concentration of 2.5×10^5 mL^{-1} in IMDM medium supplemented with 10% FBS, 1% penicillin/streptomycin, 1% HEPES, and 50 µM 2-mercaptoethanol in the presence of 20 ng mL^{-1} mGM-CSF. Half of the medium was exchanged on day 3 and day 6 and replaced with fresh complete IMDM with 20 ng mL^{-1} mGM-CSF. On day 8, cells were harvested by gently washing the plate with a pre-warmed medium and were run in flow cytometry to assess DC differentiation (CD11b and CD11c), hCD40 expression, and activation markers (CD86 and MHC-II).

2.11. BMDC Maturation and Activation

After eight days of differentiation of bone marrow precursors, 1×10^5 immature BMDC were plated per well in a 96-well TCT plate (Standard F, Sarstedt #83.3924). Different anti-CD40 antibodies, parental or BiTag (Table 1), were added to each well in a concentration ranging between 100–0.08 nM. BMDC were cultured for 48 h in IMDM medium with 20 ng mL^{-1} mGM-CSF before the supernatant was collected for IL-12 ELISA. Tests were run in duplicates.

2.12. In Vitro T Cell Activation/Expansion Assays (B3Z/pmel/OT-II)

After eight days of differentiation of bone marrow precursors, 25 000 immature BMDC were plated per well in a 96-well TCT plate (Standard F, Sarstedt #83.3924). Different concentrations of the SLPs UU5 and UU10 (for B3Z assay), UU30 (for pmel assay), or UU60 (for OT-II assay) (Table 2) with a different combination of the test anti-CD40 antibodies (Table 1) were added to the immature BMDC culture. After 24-hour incubation (2-hour incubation for UU60, with minimal disturbance of the cells, the supernatant containing the peptide/antibodies mix was removed, and the wells were washed by centrifugation twice with a pre-warmed IMDM to remove any remaining unbound peptide/Ab mix. For the T cell activation assay (B3Z assay), B3Z cells were co-cultured with BMDCs, and the co-culture was incubated for a further 24 h before the cells were lysed by adding the lysis β-mercaptoethanol buffer supplemented with the substrate CPRG. Cells were lysed to allow the β-galactosidase enzymatic activity to break down CPRG and lead to color change corresponding to the level of B3Z cell activation. Absorbance was read at 595 nm after 6 h. A positive control short peptide (SIINFEKL) (1 µM) was included in all experiments that activate B3Z and result in saturation of the colorimetric reaction and the absorbance readout. For the T cell expansion assay (pmel and OT-II assays), carboxyfluorescein succinimidyl ester (CFSE) (Thermo-Fisher) labeled pmel-1 or OT-II cells were co-cultured with BMDCs, and the co-culture was incubated at 37 °C/5% CO_2 for further 72 h before the pmel-1 cell expansion and activation were assessed using flow cytometry.

2.13. CD14$^+$ Monocyte and Peripheral blood mononuclear cells (PBMCs) Isolation, Human T Cell Expansion Assay

PBMCs were isolated from Buffy Coats, donated from healthy volunteers, by Ficoll separation using SepMate (Stemcell Technologies) together with cell density gradient Ficoll Paque Premium (GE Healthcare) according to the manufacturer's protocol. Furthermore, CD14$^+$ monocyte separation was performed with MACS human CD14 microbeads isolation kit (Miltenyi Biotec). Isolated CD14$^+$ cells were cultured for six days in complete RPMI 1640 medium with GlutaMAX, supplemented with 10% FBS, 1% of 100 IU/mL penicillin/streptomycin, 1% HEPES 1 M and 0.2% β-mercaptoethanol 50 mM (Gibco), along with 150 ng mL^{-1} hGM-CSF and 50 ng mL^{-1} hIL-4 (Peprotech) to drive differentiation into immature DCs. Half of the medium was exchanged every 2–3 days, supplemented with 150 ng mL^{-1} hGM-CSF and 50 ng mL^{-1} hIL-4 for the total volume medium. Immature monocyte-derived dendritic cells (moDC) were pulsed with the UU44 peptide, an fTag-CMV pp65 – HLA-A*0201 (NLVPM-VATV), for 24 h in the presence or the absence of the

© 2022 The Authors. Advanced Therapeutics published by Wiley-VCH GmbH

BiTag or parental anti-CD40 antibodies. The cells were washed twice by centrifugation before the autologous T cell fraction of the buffy coat, isolated with a pan T cell purification kit (Miltenyi Biotec), was co-cultured with the pulsed moDC for seven days. CMV pp65-specific T cell expansion was assessed by flow cytometry using HLA-A*02:01 CMV pp65 tetramer (Clone: T01009) (MBLinternational).

2.14. Peptide Uptake and Intracellular Release

To study BiTag platform-mediated peptide uptake and intracellular release, the FITC-labeled peptide UU44 and the BiTag antibody Bi17-CP were used. In brief, UU44 has FITC attached to the N-terminal of the peptide as an fTag that is quenched when bound to the anti-FITC scFv of Bi17-CP. A pre-mixed UU44/Bi17-CP mixture, where FITC is quenched by binding to scFv, was incubated with moDCs at 37 °C to allow peptide/antibody uptake. The uptake process was terminated at the time points: 5 min, 0.5 h, 1 h, 2 h, 4 h, or 6 h by adding ice-cold PBS and keeping the cells on ice. The cells were washed to remove excess UU44. Trypan blue was used to quench (Q) the FITC signal to discriminate the extracellular FITC signal from the intracellular signal of UU44. The amount of intracellularly released (free) UU44 was quantified as a percentage of fluorescent cells using flow cytometry for each time point.

2.15. In Vivo T Cell Expansion Experiment

Adult C57BL/6 mice (18–20 g weight) were used for in vivo antigen uptake and T cell expansion model. Groups of C57BL/6 mice (6-10 mice) received 9–11 × 10^6 CFSE-labeled pmel-1 cells intravenously (i.v.) via tail vein injection and 1–3 × 10^5 tghCD40 or WT immature BMDC (right side footpad injection) on day 0. On day 1, different combinations of BiTag or parental anti-CD40 antibodies and the hgp100 containing pTag-Ag UU-30 or the control short hgp100 peptide UU33 (Table 2) were injected on the right-side hock to investigate the peptide uptake in vivo. After 3–6 days, the draining popliteal, draining inguinal, non-draining inguinal lymph nodes and spleens were harvested and passed via 70 μm cell strainers to achieve single-cell suspensions. Pmel-1 cell accumulation and activation were assessed in the lymph nodes and spleens by flow cytometry staining of CD90.1 and the T cell activation marker ICOS.

2.16. Flow Cytometry

The following anti-mouse fluorescent-labeled antibodies from BioLegend were used for flow cytometry (clone): anti-CD11c (N418), anti-CD11b (M1/70), anti-CD90.1 (OX-7), anti-ICOS (C398.4A), anti-I-A/I-E (M5/114.15.2), anti-CD86 (GL-1), anti-hCD40 (5C3) (from BD), anti-CD45 (30-F11), anti-CD3 (17A2), anti-CD4 (RM4-4), and anti-CD8 (53-6.7). The following anti-human fluorescent-labeled antibodies from BioLegend were used for flow cytometry (clone): anti-CD3 (UVHT1), anti-CD8 (SK1), anti-CD56 (NCAM), anti-TNFα (Mab11), and anti-IFNγ (4S.B3). For flow cytometry staining, 1–5 × 10^5 cells were pelleted in flow cytometry tubes/plates by centrifugation before the antibody staining cocktail was added to the cells. Cells were incubated at 4 °C for 20 min before being washed in PBS/1% BSA. A fixation/permeabilization step was performed using Cytofix/Cytoperm solution (BD) for intracellular cytokine staining. Cells were run in CytoFLEX Flow Cytometer (Beckman Coulter Life Sciences).

2.17. IL-12 ELISA

ELISA plates (Sarstedt 82.1581.200) were coated with purified anti-mouse IL-12 antibody (clone C15.6, BioLegend) overnight at 4 °C. Plates were blocked in PBS/1% BSA before diluted supernatant was added to the ELISA plate. Thereafter, secondary biotinylated anti-mouse IL-12 (clone C17.8, BioLegend) was added before Streptavidin/HRP (Code no. P0397, Dako) was incubated in the plate. Lastly, the ELISA reaction was developed by adding TMB buffer (34 028, Sigma), and the reaction was stopped by adding 1 M sulfuric acid. Absorbance was read at 450–570 nm.

2.18. Whole Blood Loop Assay (WBLA)

Blood loop experiments were performed as described previously.[21] In brief, whole blood samples were collected from healthy blood donors, and the blood was added to surface heparinized PVC loops together with the peptide/antibody of interest in the presence of brefeldin-A. The blood loops were attached to a circulating wheel to allow the blood to be in motion and prevent coagulation. After 4–6 h of incubation at 37 °C, the blood was collected, the red blood cells were lysed, and the blood samples were stained and analyzed with flow cytometry for intracellular cytokine release.

2.19. Ethical Considerations

All animal studies were approved by Uppsala regional ethical committee (ethical approval for animal experiments Dnr: C304214/16 (C42/14) and 5.8.18-02686/2019), and all human blood experiments were approved by Uppsala regional ethical committee (DNR 2017/165 and DNR 2018/206). Informed consent of all participating subjects was obtained.

2.20. Data and Statistical Analysis

Flow cytometry data were analyzed by FlowJo, LLC. GraphPad Prism 7 was used to plot the graphs and to perform statistical analysis. The sample size for the in vivo experiments was 3–14 animals per treatment group. All data are presented as mean ± SEM. Unpaired two-tailed non-parametric Mann–Whitney test or Kruskal Wallis test with Dunn's post-test were used to assess significant differences and obtain *p*-values.

3. Results

3.1. ADAC Design and Characterization

Targeting CD40 enhances DC antigen uptake and presentation to T cells, including cross-presentation to $CD8^+$ T cells.[22] Herein,

© 2022 The Authors. Advanced Therapeutics published by Wiley-VCH GmbH

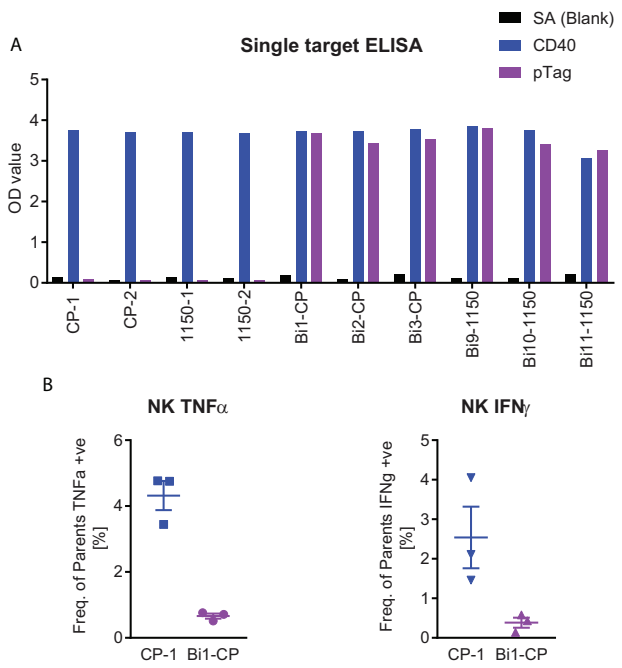

Figure 2. Target binding and FcγR mediated NK cell activation. A) Target binding was assessed by ELISA for the BiTag antibodies and their counterpart parental anti-CD40 antibodies (see Table 1). The antibody constructs were analyzed on microtiter plates coated with CD40-biotin-streptavidin (CD40, blue), UU24-biotin-streptavidin (pTag, magenta), or streptavidin only (SA, black). OD values (Abs 450 nm, y-axis) are the average of duplicates. B) NK cell activation following stimulation of whole human blood with Bi1-CP or the counterpart parental CP-1. Data are shown as mean +/−SEM.

a peptide delivery platform called ADAC was designed to contain a tetravalent bispecific antibody targeting CD40 and a peptide tag moiety, also called pTag. The bispecific antibody, also named BiTag, consists of a fully human agonistic anti-CD40 antibody covalently linked, via a glycine-serine peptide linker, to two identical scFv targeting the pTag (anti-pTag) (Figure 1). A set of seven BiTag constructs and four monoclonal anti-CD40 antibodies were designed and produced. Based on the literature, the roles of IgG subclass (IgG1 or IgG2), anti-CD40 antibody (CP-870893 or 1150), and the location of the anti-Tag fusion (CH3 or CL linkage) were evaluated (Figures 1A and 1B, and Table 1). The pTag-Ag is a SLP of 30–40 amino acid length consisting of two domains; a constant pTag, to which the scFv binds, and a variable peptide sequence that accommodates the antigenic epitope (Ag) of interest within a flanking sequence of amino acids. Herein, an 18-mer linear B cell epitope,[17] pTag, FITC[18] fTag, were used as the constant tag for concept evaluation (Table 2). The design of the BiTag allows for the simultaneous delivery of the agonistic CD40 signaling and the cargo antigen associated to the same DC, ensuring robust T cell activation (Figure 1C).

The biophysical characterization using SEC and DLS revealed minimal aggregation of the BiTag compared to the parental anti-CD40 antibodies (Figure S1, Supporting Information). The expressed BiTag and parental antibodies were confirmed to bind to their targets, CD40 and the pTag, by ELISA (**Figure 2**A). The BiTag antibodies bound CD40 within the same affinity range as the parental antibodies CP-870.893 or 1150, regardless of subclass or whether the scFv was fused to the antibody heavy or light chain as assessed by SPR (**Table 3**). As noted, there is a significant difference in measured K_D-values for the two CD40 constructs, likely explained by the difference in quaternary structures—the avi-tagged construct is monomeric, whereas CD40-Fc is, due to the Fc-fusion, dimeric leading to an avidity contribution. As K_D is used to describe the strength of a monovalent interaction, the report herein rather includes the apparent affinity (denoted as $^{app}K_d$) for the binding to CD40-Fc. As CD40 clusters on the cell surface, one may argue that the reported $^{app}K_d$ is more relevant for describing how these antibodies would interact with the target on cells, both in vitro and in vivo. SPR measurements also confirmed a high affinity for the synthetic peptide and the anti-pTag scFv in the form of BiTag (Table 3). The measured kinetic parameters are similar between the different BiTag and also very similar to values previously obtained for the scFv in soluble format (data not shown).

Importantly, using both ELISA and SPR-based sandwich experiments, BiTag antibodies were shown to simultaneously bind both their respective cognate targets (Figure S2, Supporting Information). Furthermore, SPR analyses indicated that the position of the scFv had no or minimal effect on the binding to FcRn. In contrast, a decrease in binding of a majority of the BiTag antibodies to Fcγ receptors analyzed was observed (**Table 4**). Most inhibition of binding was observed for FcγRIIIB, followed by FcγRIIA, while the least reduction in binding of the three was observed for FcγRIIIA. It should be noted that the overall kinetic profiles of the interactions to the FcγR do not seem to be affected when comparing the binding of the BiTag to its corresponding parental antibody. It is merely the level of response that changes (data not shown).

Next, a WBLA[17,21,23] was used to study the BiTag antibodies interaction with FcγRIIIA on natural killer (NK) cells using whole human blood. The WBLA has previously been shown to provide information on the interaction between monoclonal antibodies and the FcγRIIIA on NK cells, resulting in NK cell activation and cytokine release.[23] Using this system, two distinct profiles were noted based on antibody subclass, with NK cell activation taking place with IgG1 subclass but not IgG2 (Figure S3, Supporting Information). Although the SPR analyses indicated a retained FcγRIIIA binding for the BiTag of IgG1 subclass, Bi1-CP (Table 4), the parental CP-1 induced NK cell cytokine production in the WBLA, while the BiTag counterpart Bi1-CP did not (Figure 2B). This indicates that SPR analyses should always be complemented with biological readouts to fully understand the nature of how a bispecific antibody interacts with other cells.

3.2. Stability and DC Internalization of BiTag Platform Coupled Antigenic Peptide

Naked unmodified therapeutic peptides are fragile drug entities. To evaluate peptide half-life, intact pTag-Ag was evaluated over time in mouse and human plasma. This was performed using an in vitro stability experiment using the peptides UU05, UU23, and UU30 in PBS (pH 7.5) with 2% BSA and in plasma derived from mice or humans. During a 17-hour experiment, all three peptides had a half-life of ≈4 h up to no observed degradation in

© 2022 The Authors. Advanced Therapeutics published by Wiley-VCH GmbH

Table 3. SPR analyses of target binding of parental and BiTag antibodies. The reaction rate kinetics constants (association rate constant [k_a [M^{-1} s^{-1}]], dissociation rate constant [k_d [s^{-1}]], and equilibrium of dissociation [K_D [nM]]) were calculated based on a 1:1 kinetic binding model for all interactions except for 1150-based antibody constructs together with CD40-avi. Here, the steady state binding model was used to get an estimation of K_D. For binding to CD40-Fc, the k_a and k_d contain an avidity component due to the dimeric nature of the antigen. Therefore, the apparent affinity constant ($^{App}K_D$) is used to describe these interactions.

	Binding to CD40-Fc			Binding to CD40-avi			Binding to pTag-Ag (UU30)		
Antibody	$^{app}K_D$ [nM]	k_a [1/Ms]	k_d [1/s]	K_D [nM]	k_a [1/Ms]	k_d [1/s]	K_D [nM]	k_a [1/Ms]	k_d [1/s]
Bi1-CP	0.14	2.3E+05	3.1E-05	15	8.4E+04	1.2E-03	1.0	5.3E+05	5.4E-04
Bi2-CP	0.16	1.9E+05	2.9E-05	14	8.6E+04	1.2E-03	0.9	6.0E+05	5.4E-04
Bi3-CP	0.12	2.4E+05	2.8E-05	14	7.8E+04	1.1E-03	0.9	4.8E+05	4.3E-04
Bi9-1150	1.5	2.7E+06	3.9E-03	1000 ± 300	–	–	0.9	5.8E+05	5.4E-04
Bi10-1150	1.7	2.6E+06	4.3E-03	1000 ± 300	–	–	1.2	6.4E+05	7.6E-04
Bi11-1150	1.7	2.1E+06	3.7E-03	1000 ± 300	–	–	0.7	5.4E+05	3.8E-04
Bi17-CP	0.17	1.8E+05	3.0E-05	14	8.2E+04	1.2E-03	No binding detected		
CP-1	0.12	2.0E+05	2.3E-05	15	7.6E+04	1.2E-03	No binding detected		
CP-2	0.16	2.0E+05	3.1E-05	14	8.2E+04	1.2E-03	No binding detected		
1150-1	1.8	1.5E+06	2.7E-03	1000 ± 300	–	–	No binding detected		
1150-2	1.4	1.5E+06	2.1E-03	1000 ± 300	–	–	No binding detected		

Table 4. Normalized binding response of the BiTag antibodies to FcRn and to three different FcγR; FcγRIIIA (CD16a), FcγRIIIB (CD16b), and FcγRIIA (CD32a). The binding response values were normalized based on the signal obtained for respective parental IgG to each of the different Fc receptors, and this value was set to 100%. The binding response for each sample was taken at the end of the association phase. ++ indicates a normalized binding response ≥80%, + indicates a normalized binding response <80% and − indicates that no binding was detected.

Antibody	FcRn	FcγRIIA	FcγRIIIA	FcγRIIIB
Bi1-CP	++	++	++	+
Bi2-CP	++	+	–	–
Bi3-CP	++	+	++	+
Bi9-1150	++	+	++	+
Bi10-1150	++	+	–	–
Bi11-1150	++	+	++	+
CP-1	++	++	++	++
CP-2	++	++	–	–
1150-1	++	++	++	++
1150-2	++	++	–	–

PBS, 2% BSA (Figure S4, Supporting Information). Compared to PBS, considerably rapid degradation of UU30 and UU05 was noted in mouse and human plasma, respectively. The half-life for UU30 in mouse plasma was 18 min, and the half-life for UU05 in human plasma was 6 min (Figure S5, Supporting Information).

Next, peptide integrity of UU30 and UU05 was studied in mouse and human plasma, respectively, in the presence of antibodies. The peptides were incubated at 37 °C with the mouse or human plasma alone, mixed with the 1150–1 parental antibody or with Bi9-1150. In mouse plasma, the binding of UU30 to the BiTag improved peptide stability with no detectable degradation of the peptide during the 4-hour experiment. In contrast, for the peptide alone or peptide mixed with the parental anti-CD40 antibodies without binding properties to the peptide, the half-life of the peptide was measured to be ≈19.5 min (**Figure 3**A). Moreover, in human plasma, binding of the peptide UU05 to Bi9-1150 resulted in slower degradation, with a half-life of 24 min compared to an average of 13 min when UU05 was incubated in the plasma alone or with the parental antibody 1150–1 (Figure 3B). Using protease inhibitors in mouse plasma displayed a prolonged half-life from 0.4 to 3.7 h. Notably, the increased stability of the BiTag-bound peptide, in this experiment Bi10-1150, did not synergize by the addition of protease inhibitors, and the half-life of Bi10-1150 bound UU30 with and without the protease inhibitors was 6.1 and 6.4 h, respectively (Figure S6, Supporting Information). This suggests the improved peptide stability by BiTag is likely via protection from degradation by proteases.

To confirm the protective properties of the ADAC technology in vivo, intact pTag-Ag and antibody in plasma and the draining popliteal and inguinal lymph nodes of C57BL/6 mice following hock injection with the UU30 peptide, mixed with either the 1150–2 parental antibody or with the Bi10-1150 was quantified. Each mouse received a 2 mg kg^{-1} body weight of antibody with the peptide UU30 co-injected at an antibody to the peptide molar ratio of 1:2. The mice were sampled at 0.5, 1.5, 4, and 8 h after vaccination. Plasma concentrations of the antibodies in the two different groups were in a close range, ranging from 8.5–55.0 (1.7–11 μg mL^{-1}) and 18.7–126.7 nM (2.8–19 μg mL^{-1}) for Bi10-1150 and 1150–2, respectively (Figure 3C). For the pTag-Ag, in the group treated with UU30 + 1150–2, no peptide was detectable in the plasma at any time point (LLOD ≈0.2 nM). In contrast, UU30 was detected at a concentration ranging from 10–65 nM in plasma when using the Bi10-1150 delivery strategy, corresponding to 2–14% of the injected dose if the mouse plasma volume is ≈0.9 mL. This supports the BiTag's protective effect on the antibody-bound peptide in vivo (Figure 3C). The plasma Bi10-1150:UU30 ratio dropped from 1.6 at the 0.5-hour time point to 0.4 at the 8-hour time point, indicating that UU30 had a shorter half-life in plasma than the BiTag (Figure 3D).

Both 1150–2 and Bi10-1150 antibodies were detectable at similar levels, in the lymph node, with the maximum average

© 2022 The Authors. Advanced Therapeutics published by Wiley-VCH GmbH

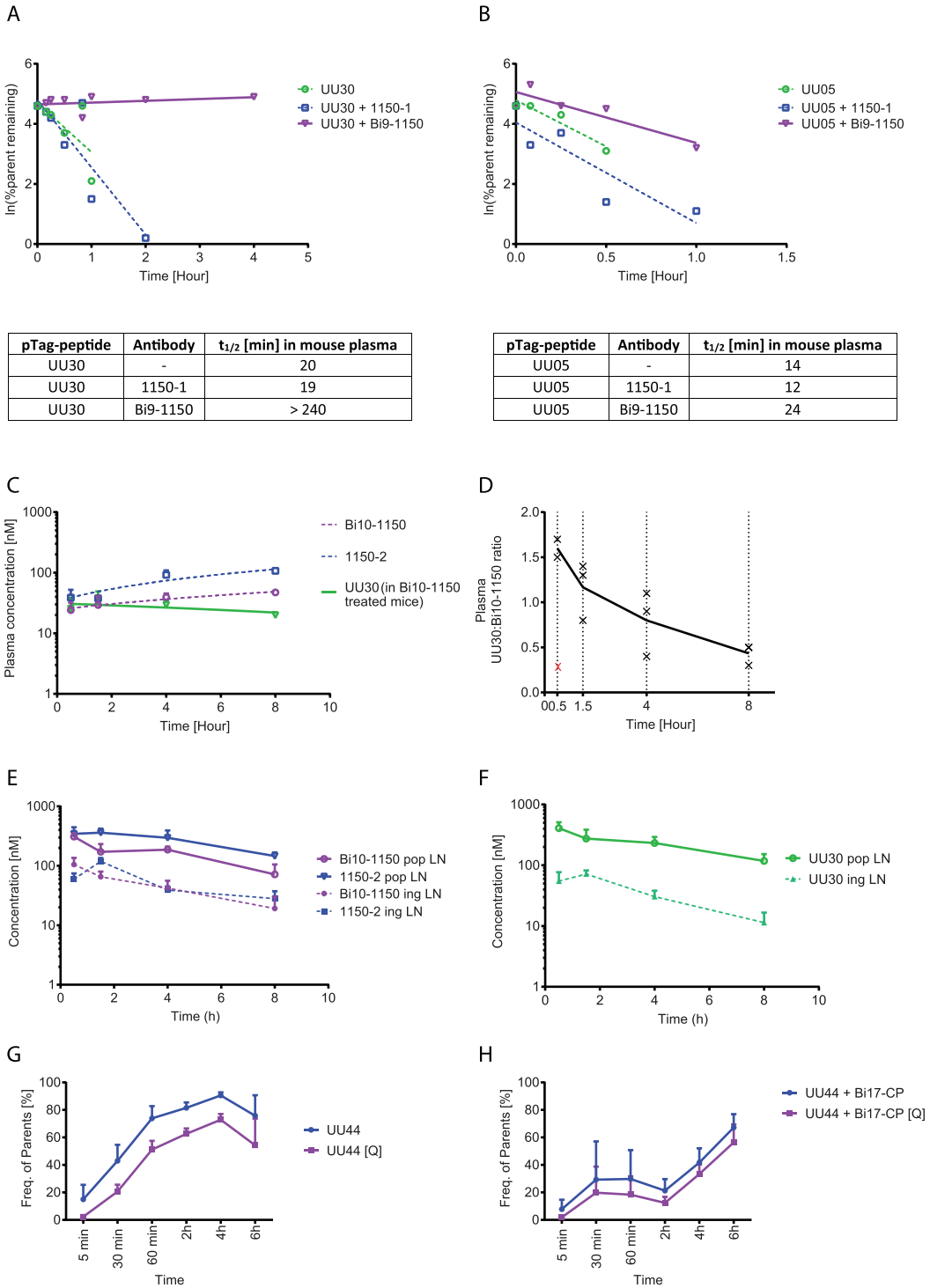

pTag-peptide	Antibody	$t_{1/2}$ [min] in mouse plasma
UU30	-	20
UU30	1150-1	19
UU30	Bi9-1150	> 240

pTag-peptide	Antibody	$t_{1/2}$ [min] in mouse plasma
UU05	-	14
UU05	1150-1	12
UU05	Bi9-1150	24

Figure 3. In vitro and in vivo peptide stability and intracellular release. In vitro peptide stability in A) mouse and B) human plasma. The pTag-peptide A) UU30 and B) UU05 were incubated for 4 h in the 37 °C plasma alone, mixed with the parental antibody 1150–1 or mixed with the BiTag antibody Bi9-1150. The remaining intact peptide concentration was detected using mass spectrometry. C) The in vivo integrity of UU30, 1150—2, and Bi10-1150 in mouse plasma were determined by mass spectrometry following vaccination in the hock at 2 mg mL^{-1} antibody and 1:2 Bi10-1150:UU30 or 1150–2:UU30 molar ratio. D) Bi10-1150:UU30 ratio in mouse plasma over time after the in vivo administration. Each dot represents the mean ($n = 3$) per time point E) Bi10-1150 and 1150–2 concentration in the draining popliteal and the draining inguinal lymph nodes following hock administrated vaccination. F) UU30 concentration in the draining popliteal and the draining inguinal lymph nodes following hock administrated vaccination with UU30 and Bi10-1150. G) Internalization kinetics for the fTag containing peptide UU44 by moDC. Trypan blue was used to quench extracellular peptides [Q]. H) Internalization kinetics for the fTag-containing peptide UU44 when complexed with the Bi17-CP by moDC. Trypan blue was used to quench extracellular peptides [Q]. Dots represent the mean. Error bars represent SEM. ln = natural log, BSA = bovine serum albumin, LN = lymph node, pop = popliteal, ing = inguinal.

© 2022 The Authors. Advanced Therapeutics published by Wiley-VCH GmbH

concentration of 344.8 ± 172.7 and 309.8 ± 72.6 nM in the popliteal lymph node 0.5 h after administration for 1150–2 and Bi10-1150, respectively (Figure 3E). However, UU30 was only detected in the group treated with Bi10-1150, both when analyzing the popliteal and the inguinal lymph nodes (Figure 3F).

Next, peptide internalization and release were investigated when delivered by the ADAC strategy. A FITC tagged CMV $pp65_{495\text{-}503}$ (NLVPMVATV) peptide (fTag-NLV; UU44) was used to study the release of the cargo over time inside APC. A BiTag version Bi17-CP, which has the anti-fTag as a scFv, was used. First, the binding of Bi17-CP to the UU44 was confirmed by demonstrating that the Bi17-CP quenches the fluorescence signal upon fTag-Bi17-CP interaction (Figure S7, Supporting Information). To investigate the internalization kinetics, human moDCs were pulsed with the UU44 peptide either alone or when bound to Bi17-CP. The fluorescence signal was assessed when cells were stained with trypan blue to quench any extracellular fluorescent signal (UU44 [Q]) or without quenching the extracellular signal (Figure 3G,H). Pulsing the moDCs with UU44 alone resulted in a steady increase of the intracellular fluorescence with time, indicating the cells' continuous uptake in a closed system where peptides are not eliminated as would be the case in vivo (Figure 3G). When complexed with the BiTag Bi17-CP, the fluorescent signal of UU44 was initially low (quenched). After 2 h, the fluorescence increased steadily, indicating intracellular dissociation and release of the fTag-peptide from Bi17-CP takes place after 2 h and continues to be released up to 6 h (Figure 3H).

3.3. The BiTag Platform Activates DC and Enhances Antigen Uptake and Presentation In Vitro

To evaluate the agonistic property of the different BiTag and parental antibodies, BMDC from a tghCD40 mouse strain were used.[10] By stimulating immature BMDCs (imBMDCs), it was apparent that the BiTag retained the agonistic activity. Interestingly, while the 1150-based BiTag constructs showed comparable IL-12 production to their parental counterparts (**Figure 4**A), CP-870.893-based BiTag constructs induced a significant increase in DC IL-12 production compared to the parental CP-870.893 antibodies (Figure 4B,C).

Furthermore, while IgG2 isotype induced higher agonistic activity and IL-12 production in the format of the parental antibody, compared to the IgG1 format, this difference was less clear when comparing IgG1 and IgG2 of the BiTag versions of the antibody. Although puzzling, this effect could be attributed to changes in FcγR interaction that could be potentially induced by linking the scFv to the antibody backbone or clustering of the antibodies on the cell surface or an inherited feature unique to the transgenic BMDCs. An experiment to compare aggregated and 99% monomeric fractions of the bispecific antibodies was also performed to determine whether aggregation had any role in the results. There was no difference in the agonistic activity between aggregated and pure monomeric antibodies in the cell assay (data not shown). Of note, agonistic IL-12 stimulation was not observed when treating WT BMDC that lack human CD40 (Figure S8, Supporting Information); also supporting that there was no non-target mediated protein aggregation causing the stimulation.

T cell activation was studied by co-cultured tghCD40 BMDC with B3Z hybridoma cells.[14] Treatment of tghCD40 BMDCs with a mixture of BiTag antibodies and the pTag-Ag UU05, which is a pTag-OVA(SIINFEKL) (Table 2) mixture resulted in a substantial increase in $CD8^+$ T cell activation compared to treating the cells with the antigen UU05 alone (Figure 4D,E). Mixing parental agonistic anti-CD40 antibodies CP-1, CP-2, 1150–1, and 1150–2 with UU05 did not improve antigen presentation and T cell activation. Besides the pTag-Ag UU05, a B3Z co-culture with the BiTag antibodies with UU25, a whole OVA protein conjugated with a pTag at OVA:pTag of 1:4 ratio, or with the SLP UU10 that include the antigenic epitope SIINFEKL but lacks the pTag, was performed. Like UU05, pTag/UU25 combination displayed a synergistic activity and induced higher T cell activation compared to treatment with UU25 alone or with parental agonistic CD40 antibodies (Figure 4F). In contrast, BiTag antibodies had no added effect on T cell activation when a non-pTag containing peptide (UU10) was used as the antigenic peptide emphasizing the critical role of the pTag in facilitating the CD40 mediated antigen uptake (Figure 4G). To further verify the CD40-dependent peptide uptake, WT BMDCs that lack hCD40 as the target were used, where no DC activation or T cell proliferation was noted by UU05/BiTag stimulation (Figure 4H).

Although $CD8^+$ T cells can be cross-primed by DCs on many occasions, like viral infections,[24] $CD4^+$ T cells are crucial to support long-lasting, effective cytotoxic and memory $CD8^+$ T cell responses.[25] To explore the flexibility of the platform, murine tghCD40 BMDC or human moDCs were pulsed with a different set of pTag-Ag, UU60 and UU44. These pTag-Ag include the ovalbumin $OT\text{-}II_{323\text{-}339}$ CD4 epitope or the CMV pp65 $NLV_{495\text{-}503}$ CD8 epitope, respectively. In the OT-II model, the pulsing of BMDC with UU60 in the presence of Bi10-1150 resulted in an apparent increase in OT-II specific $CD4^+$ T cell proliferation and upregulation of the expression of the activation marker ICOS (Figures 4I and 4J). Notably, the pulsing of the BMDCs with the pTag-SLP containing irrelevant epitope did not induce any $CD4^+$ T cell proliferation (data not shown). In the CMV model, Bi17-CP treatment enhanced the NLV-specific $CD8^+$ T cells (Figure 4K). Notably, the parental antibody CP-2 resulted in a comparable response to the BiTag version of the antibody, likely because this peptide has an inherent long half-life and as the closed nature of the in vitro system does not provide other sources of eliminations pathways than degradation, there is no added benefit by the BiTag in this specific setup with this specific peptide. The co-stimulation dependence of the assay, in contrast to the B3Z assay that is co-stimulation independent, might have also played a role when excess antigen is present.

3.4. The BiTag Platform Enhances Peptide-Specific T Cell Proliferation and Activation In Vivo

Next, the in vitro T cell expansion and activation of gp100 specific $CD8^+$ T cells (pmel-1) were assessed when tghCD40 BMDCs were pulsed with the pTag-Ag UU30 that contains hgp100 as an antigen. The presence of either the parental or the BiTag antibodies enhanced the pmel-1 activation in vitro (**Figure 5**A). Because of the noted in vitro system's limitation, being a closed system not mimicking the in vivo situation where the molecular weight

© 2022 The Authors. Advanced Therapeutics published by Wiley-VCH GmbH

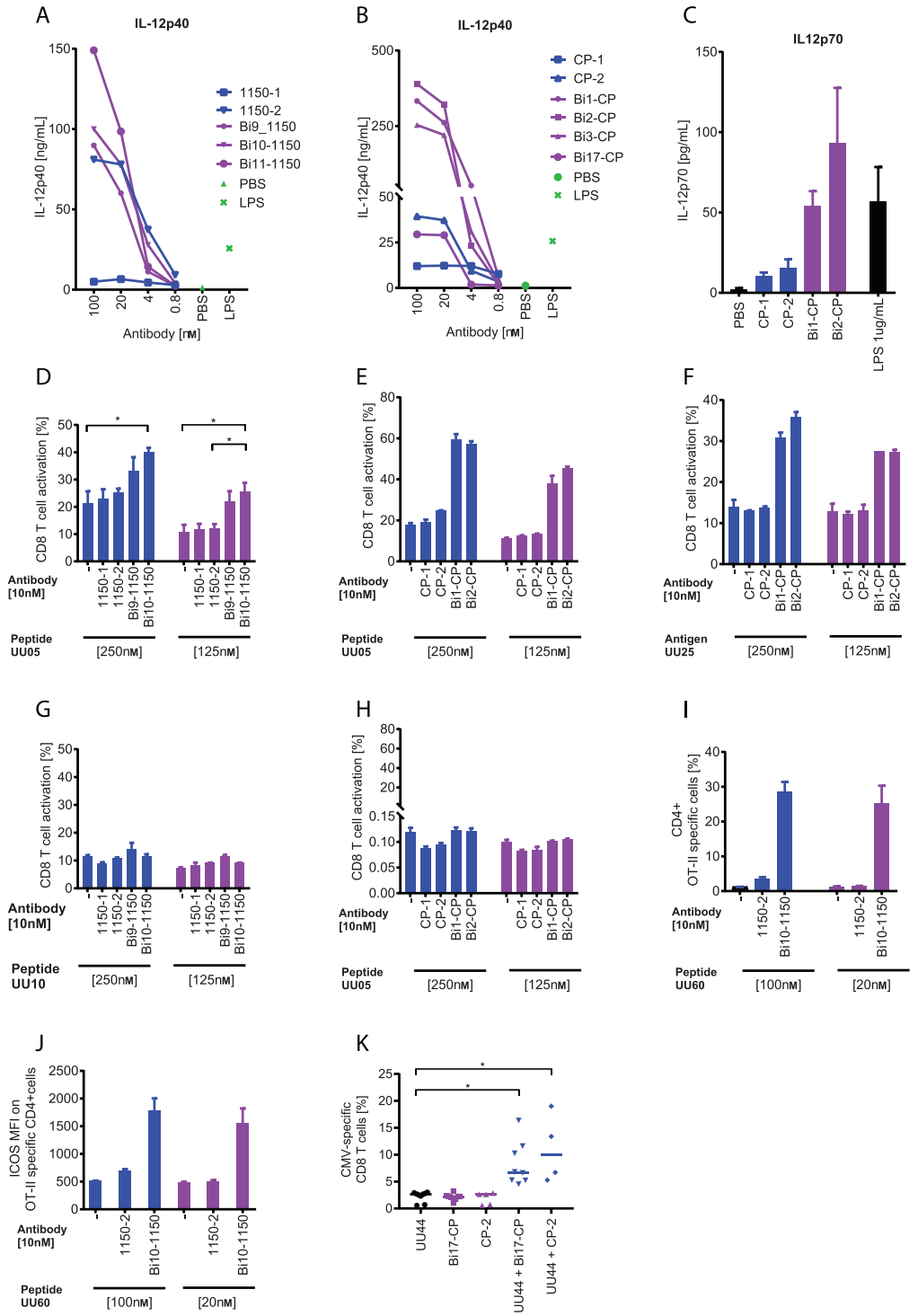

Figure 4. In vitro agonistic activity and antigen uptake enhancement by the BiTag platform. A–C) imBMDC from tghCD40 were treated with BiTag or parental antibodies for 48 h. IL-12p40 (A,B) or IL12p70 (C) concentrations were measured in the supernatant by ELISA 48 h after tghCD40 BMDC treatment or LPS. D–G) tghCD40 BMDC were treated with UU-05 (D,E), UU25 (F), or UU-10 (G) in the presence or absence of BiTag or parental antibodies. After 24 h, unbound treatments were washed and DCs were co-cultured with B3Z cells. B3Z cell activation was quantified after a further 24 h via measuring the colorimetric change in CPRG substrate as described in the Experimental Section. "CD8 T cell activation [%]" refers to the fraction of T cells activated in reference to the positive control, which saturates the colorimetric reaction at 100% activation. H) B3Z cell activation assay when wild type BMDC was pulsed with UU05 in the presence of BiTag or parental antibodies. I,J) Transgenic $CD4^+$ T cell proliferation (I), and ICOS expression (J) after co-culturing the T cells with OT-II pulsed tghCD40 BMDC with the pTag-OT-II peptide UU60. K) CMV specific $CD8^+$ T cell proliferation after co-culturing the T cells with UU44, a pTag containing CMV pp65 $NLV_{495\text{-}503}$ CD8 epitope, pulsed moDCs in the absence or the presence of BiTag or parental antibodies ($n = 4$–8). Dots represent the mean. Error bars represent SEM. * = $p < 0.05$, Kruskal Wallis test with Dunn's post-test.

© 2022 The Authors. Advanced Therapeutics published by Wiley-VCH GmbH

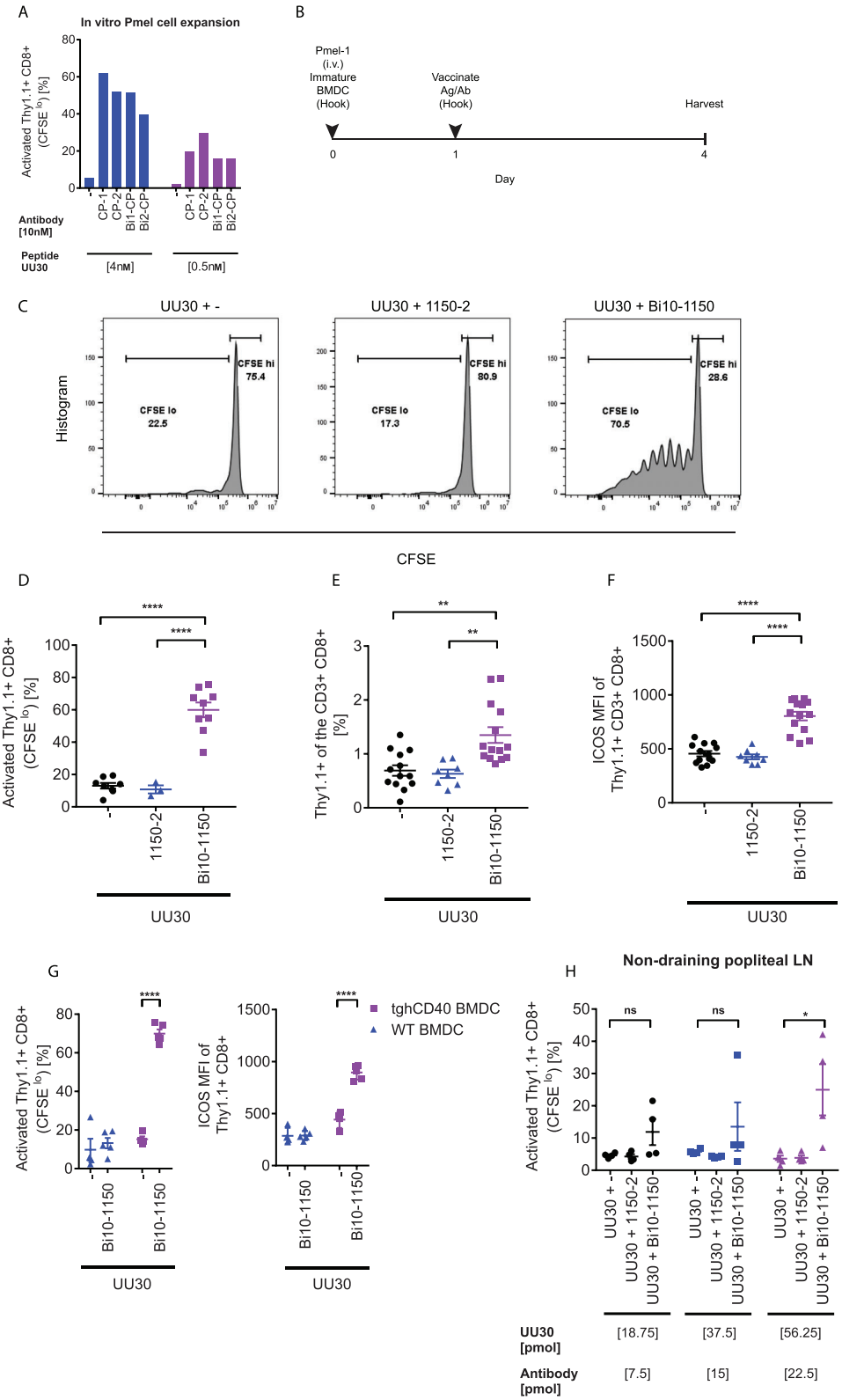

Figure 5. BiTag induces robust antigen-specific CD40-dependent CD8$^+$ T cell expansion and activation in vivo. A) In vitro activation and proliferation of the CFSE-labeled congenially marked thy1.1 Pmel-1 CD8$^+$ T cells when co-cultured with the tghCD40 BMDC were treated with UU30 peptide in the presence or the absence of BiTag or parental antibodies. After 24 h, unbound treatments were washed and DCs were co-cultured with pmel-1 CD8$^+$ T cells. Pmel-1 cell proliferation was quantified after a further 72 h. B) tghCD40 BMDC and CFSE-labeled thy1.1$^+$ Pmel-1 cells were transferred into the hock and intravenously, respectively. Mice were vaccinated with the peptide antigen UU30, UU30+Bi10-1150, or UU30+1150-2 in the same side hock

© 2022 The Authors. Advanced Therapeutics published by Wiley-VCH GmbH

will determine the dispersion of the compounds, the activity of the BiTag platform was assessed in vivo using the pmel-1 model. CFSE-labeled pmel-1 cells were administrated by intravenous tail vein injection, and tghCD40 BMDCs were injected in the hock of C57BL/6 mice. The IgG2-based Bi10-1150 and 1150–2 were chosen for this experiment due to the uniform DC activation profile of the bispecific and parental antibodies and the superior T cell activation in vitro, along with literature supporting the IgG2 format for agonistic activity.[26–29] A mixture of UU30 and Bi10-1150 or 1150–2 was injected to the same side hock that received the tghCD40 BMDCs (Figure 5B). Draining popliteal lymph node analysis after 72 h of treatment identified an average of 60% expansion of pmel-1 (Thy1.1$^+$, CD3$^+$, CD8$^+$) cells in the UU30/Bi10-1150 group (Figure 5C–E). Similarly, the superiority of the BiTag in inducing antigen-specific T cell expansion was observed with Bi1-CP and Bi2-CP (Figure S9, Supporting Information). Besides this, ICOS was upregulated on the antigen-specific T cells in the group treated with UU30/Bi10-1150 combination compared to UU30 monotherapy or UU30/1150-2 in combination (Figure 5F). To confirm the CD40 dependence of the antigen uptake, the setup was repeated by transferring CFSE-labeled pmel-1 and WT BMDCs lacking the target hCD40 to the mice. Bi10-1150 did not induce Pmel-1 expansion or activation when WT BMDCs were transferred (Figure 5G). Furthermore, this experiment was repeated with increasing UU30 and antibody mix concentrations to investigate dose-dependent responses. There was no notable difference in the local pmel-1 cell activation/proliferation in the draining popliteal lymph node (Figure S10, Supporting Information). However, with the higher dose (56.25 pmol/22.5 pmol UU30/Bi10-1150), a significantly enhanced pmel-1 proliferation in the non-draining popliteal lymph node (Figure 5H) was noted. No pmel-1 cell proliferation or activation in the spleen was apparent at any doses. Together, these results demonstrate the in vivo CD40-dependent improved DC antigen delivery and presentation by the BiTag platform and that the effect is mainly localized, supporting the safety aspect of the therapy. T cell migration and tumor targeting will occur regardless of whether the priming and expansion are induced locally.

4. Discussion and Conclusion

Agonistic anti-CD40 antibodies have shown promising anticancer effects in pre-clinical evaluations via T cell-dependent[22,30] or T cell-independent mechanisms.[31,32] In the clinic, the maximum tolerated dose (MTD) is limited to ≈0.3 mg kg^{-1} for selicrelumab, and systemic leakage of tumor-localized, injected anti-CD40 therapy into highly vascularized tumors using mitazalimab (ADC-1013) has been shown to trigger systemic cytokine release.[33] As anti-CD40 antibodies rely on antigens for proper T cell activation in T cell-dependent anti-tumor responses, it is crucial to adapt CD40-targeting strategies. Bispecific antibody targeting strategies can be developed to target tumor antigens on the surface of the tumor cells, for example, targeting mesothelin/CD40[34,35] and HER2/CD40,[36] or surface-expressed tumor antigens that are also present on exosomes or other cellular released particles.[37] All with the ambition to couple the stimulation of CD40 with antigen presentation. However, a limitation of this strategy is its reliance on high expression of the tumor antigen to achieve effective tumor antigen-specific immune stimulation, which is not always the case and often there is a limited number of tumor-specific surface targets.[38] In addition, vesicles/exosomes that carry tumor material are also potentially immunosuppressive, increasing the risk for an ineffective antigen presentation pathway.[39–41] Next-generation sequencing offers a novel pathway to individualized therapies. Synthetic peptide drugs can be synthesized per individual based on sequencing data and epitope-based algorithm prediction strategies.[9] However, the peptides' physicochemical properties will affect the synthesis, identification, purification, solubility, and half-life. An alternative to the peptide-based vaccine is the use of the more traditional whole protein vaccine strategy for broad HLA and immunological response coverage. However, whole protein vaccines come with several limitations in cancer therapeutics. DCs are less efficient in presenting and cross-presenting antigens delivered as whole proteins compared to synthetic peptides.[42,43] Additionally, targeting endogenous proteins, as whole proteins combined with adjuvants, leads to the formation of polyclonal anti-drug antibodies against the endogenous protein, which can both impact the natural biology of the endogenous protein and increase the toxicity risk of the vaccine candidate. SLPs focus on the identified neoantigen regions, can maintain a proper HLA coverage if not trimmed to a specific epitope, and are produced with the focus on inducing a T cell response. Although antibody response may sometimes develop, it is to a specific linear peptide sequence and is less likely to bind the endogenous peptide sequence as that will have an alternative conformation in the endogenous protein.[44,45]

A significant difficulty with therapeutic peptides is the in vivo stability and the rapid clearance in the blood. Several approaches have been investigated to improve peptide half-life, including chemical modification of the peptide, for example, glycosylation or acetylation of the peptide's terminal amino acids,[46] or by ovalbumin conjugation or Fc fusions.[47,48] Herein, we show that, in addition to increasing the peptide immunogenicity, the peptide-BiTag interaction enhances the peptide half-life in mouse and human plasma both in vitro and in vivo. This amplifies the bioavailability and contributes to the improved immunogenicity of the BiTag peptide vaccination. Despite the observed improved half-life of all peptides tested, we did note that the effect was peptide dependent. It is thus likely that both the inherent stability of each peptide along with sequence-specific enzymatic cleavage sites and their distance to the pTag can impact the resulting

after 24 h. Draining and non-draining popliteal lymph nodes were analyzed after 72 h. C) Representative histograms showing T cell proliferation and the resulting CFSE signal intensity reduction. D–F) Draining popliteal LN flow cytometry analysis for pmel-1 expansion measured as D) %CFSE low, E) %thy1.1$^+$, and F) pmel-1 cell activation measured by ICOS expression (n = 3–14, data are pooled from 3 independent experiments). G) Comparison of pmel-1 cell expansion and activation in draining popliteal lymph node when WT versus tghCD40 BMDC are transferred to the hock (n = 4). H) Flow cytometry analysis of pmel-1 proliferation at the non-draining popliteal lymph node at antibody doses (7.5, 15, and 22.5 pM). The peptide is given at 2.5× of the antibody molar concentration. Data are shown as mean +/−SEM. * = $p < 0.05$, ** = <0.01, *** = $p < 0.001$, **** = $p < 0.0001$, Kruskal Wallis test with Dunn's post-test or Mann–Whitney test.

© 2022 The Authors. Advanced Therapeutics published by Wiley-VCH GmbH

half-life either as a naked peptide or when in complex with the BiTag. Importantly, the superior BiTag responses are dependent on CD40-mediated uptake. Therefore, the dual effects of the CD40-mediated peptide uptake and half-life improvement result in the noted superior expansion of T cells using the ADAC approach. Bonifaz et al.[49] have shown earlier that antibody-mediated targeting of antigens to dendritic cells via DEC205 leads to tolerance rather than T cell activation in the absence of adjuvant, which one can overcome by adding CD40 agonistic stimulation, herein features that are combined in the form of dual delivery and adjuvant capacity by using the ADAC technology.

The agonistic anti-CD40 antibodies rely on the IgG2 format and the unique disulfide hinge for retained agonistic activity.[26–29] However, IgG1 formats are also employed, taking advantage of the FcγR interaction to deliver agonistic anti-CD40 signaling.[26,50] While BiTag antibodies of IgG1 format (e.g., Bi1-CP) appeared to retain their FcγRIIIA interaction in the SPR experiment, the human whole blood experiment indicated that the FcγRIIIA interaction was impaired, possibly by steric hindrance on cell surfaces by the presence of the scFv. Notably, however, the Fc interaction of BiTag with FcγRIIIB, and to some extent, FcγRIIA, appeared to be attenuated. Nonetheless, we observed no apparent differences between BiTag of IgG1 or IgG2 format in relation to agonistic activity when using murine tghCD40 BMDC. In contrast, when using human moDCs, the IgG2 format was superior to the IgG1 (data not shown), which is in line with previous studies.[26,29] Based on agonistic data and because Fc receptor interaction in trans may hamper antibody internalization, an Fc independent agonistic effect as IgG2 is preferred in our case. However, the antibody isotype and the interaction with FcγR warrant further investigation to evaluate the BiTag signaling via FcγR, and the toxicity implications, such as target cell depletion, related to FcγR interaction following anti-CD40 infusion or intratumoral administration.[33,51] It is also known from the literature that the IgG2 isotype is not entirely Fc inert, as it can cross-link human FcγRIIA when antibodies are bound to a target and the Fc part is presented in a complexed form,[52] also supported by our own data herein. This should be taken into account when improving cargo delivery to cells via the ADAC technology ahead.

Our study is not without limitations. The comparison between the BiTag platform and the parental agonistic anti-CD40 antibodies in vitro, where the antigens and antibodies are available in excess and do not follow the physiologic pharmacokinetics, including distribution and elimination, makes direct comparison challenging. In vitro BiTag-induced T cell activation was observed with all the in vitro models we tested. However, the superiority of the BiTag platform relative to the parental anti-CD40 was best studied in vivo when the peptides and the antibodies follow physiologic pharmacokinetics, where elimination of smaller molecular weight substances is rapid. Additionally, despite BiTag displaying superior antigen uptake and presentation by DCs in vivo, our in vivo model was based on adoptive transfer of transgenic human CD40 BMDCs, which limited characterization of the other critical APCs, B cells, and macrophages. Further analysis of these critical cell populations and the mode-of-action of the ADAC technology is thus warranted in human CD40 transgenic mice and by the use of humanized model systems.

In summary, the ADAC platform provides a means for flexible peptide-based therapeutic vaccines tailored for individualized cancer therapy. The increased immunogenicity and stability of the peptides using this strategy enable a local low dose of administration of the anti-CD40 antibody in conjunction with tumor antigens. The ADAC platform removes the constraint of an intratumoral injection in deep tumor lesions, the risk of expanding myeloid suppressor cells in the tumor, as well as the toxicity profile of the intravenous infusion. It also provides antigens in cases where tumor antigen release is not sufficient. This promising pre-clinical proof-of-concept and characterization of this novel bispecific approach justify further clinical development of this approach to study its effects in treating human cancer.

Supporting Information

Supporting Information is available from the Wiley Online Library or from the author.

Acknowledgements

The authors thank Peter Ellmark and Adnan Deronic (Alligator Biosciences, Lund, Sweden) for providing bones to prepare bone marrow dendritic cells from the transgenic human CD40 mouse strain. They thank all the blood donors for their contribution in providing them with blood samples. They thank the financial support from the Swedish Society for Medical Research and Knut and Alice Wallenberg Foundation as well as SweLife/Vinnova, all to S.M.M.

Conflict of Interest

S.M.M. is a co-founder of Immuneed, Vivologica, and Strike Pharma and holds shares in the above companies. M.E., I.L., and M.L. are co-founders and shareholders in Strike Pharma. S.M.M. and M.E. are shareholders in Ultimovacs ASA, and S.M.M. is also an employee of Ultimovacs AB. None of the companies have had any influence over the work nor have contributed financially to the work presented herein.

Data Availability Statement

The data is freely available and is already provided in the manuscript as a whole.

Keywords

Antibody Drug Affinity Conjugate (ADAC), cancer vaccine, cargo delivery, CD40, immunotherapy, multivalent antibodies, synthetic peptides

Received: February 6, 2022
Revised: April 4, 2022
Published online: June 14, 2022

[1] T. R. Pearce, K. Shroff, E. Kokkoli, *Adv. Mater.* **2012**, *24*, 3803.
[2] C. D. Spicer, C. Jumeaux, B. Gupta, M. M. Stevens, *Chem. Soc. Rev.* **2018**, *47*, 3574.
[3] S. D. Xiang, K. L. Wilson, A. Goubier, A. Heyerick, M. Plebanski, *Front. Immunol.* **2018**, *9*, 2968.
[4] A. de Mare, A. J. A. Lambeck, J. Regts, G. M. van Dam, H. W. Nijman, H. Snippe, J. Wilschut, T. Daemen, *Gene Ther.* **2008**, *15*, 393.

© 2022 The Authors. Advanced Therapeutics published by Wiley-VCH GmbH

[5] W. Yin, L. Gorvel, S. Zurawski, D. Li, L. Ni, D. Duluc, K. Upchurch, J. R. Kim, C. Gu, R. Ouedraogo, Z. Wang, Y. Xue, H. M. Joo, J. P. Gorvel, G. Zurawski, S. K. Oh, *eBioMedicine* **2016**, *5*, 46.
[6] T. A. Barr, A. L. McCormick, J. Carlring, A. W. Heath, *Immunology* **2003**, *109*, 87.
[7] C. Hatzifoti, A. W. Heath, *Immunology* **2007**, *122*, 98.
[8] J. Carlring, M. J. Szabo, R. Dickinson, E. De Leenheer, A. W. Heath, *Blood* **2012**, *119*, 2056.
[9] Z. Hu, P. A. Ott, C. J. Wu, *Nat. Rev. Immunol.* **2018**, *18*, 168.
[10] S. M. Mangsbo, S. Broos, E. Fletcher, N. Veitonmäki, C. Furebring, E. Dahlén, P. Norlén, M. Lindstedt, T. H. Tötterman, P. Ellmark, *Clin. Cancer Res.* **2015**, *21*, 1115.
[11] L. C. Sandin, T. H. Tötterman, S. M. Mangsbo, *Oncoimmunology* **2014**, *3*, e27400.
[12] L. C. Sandin, A. Orlova, E. Gustafsson, P. Ellmark, V. Tolmachev, T. H. Tötterman, S. M. Mangsbo, *Cancer Immunol. Res.* **2014**, *2*, 80.
[13] P. Y. Pan, G. Ma, K. J. Weber, J. Ozao-Choy, G. Wang, B. Yin, C. M. Divino, S. H. Chen, *Cancer Res.* **2010**, *70*, 99.
[14] J. Karttunen, S. Sanderson, N. Shastri, *Proc. Natl. Acad. Sci. USA* **1992**, *89*, 6020.
[15] W. W. Overwijk, M. R. Theoret, S. E. Finkelstein, D. R. Surman, L. A. De Jong, F. A. Vyth-Dreese, T. A. Dellemijn, P. A. Antony, P. J. Spiess, D. C. Palmer, D. M. Heimann, C. A. Klebanoff, Z. Yu, L. N. Hwang, L. Feigenbaum, A. M. Kruisbeek, S. A. Rosenberg, N. P. Restifo, *J. Exp. Med.* **2003**, *198*, 569.
[16] M. J. Barnden, J. Allison, W. R. Heath, F. R. Carbone, *Immunol. Cell Biol.* **1998**, *76*, 34.
[17] E. A. K. Fletcher, W. van Maren, R. Cordfunke, J. Dinkelaar, J. D. C. Codee, G. van der Marel, C. J. M. Melief, F. Ossendorp, J. W. Drijfhout, S. M. Mangsbo, *J. Immunol.* **2018**, *201*, 87.
[18] E. Söderlind, L. Strandberg, P. Jirholt, N. Kobayashi, V. Alexeiva, A. M. Åberg, A. Nilsson, B. Jansson, M. Ohlin, C. Wingren, L. Danielsson, R. Carlsson, C. A. K. Borrebaeck, *Nat. Biotechnol.* **2000**, *18*, 852.
[19] C. Preger, E. Wigren, E. Ossipova, C. Marks, J. Lengqvist, C. Hofström, O. Andersson, P. J. Jakobsson, S. Gräslund, H. Persson, *J. Biol. Chem.* **2020**, *295*, 13981.
[20] J. R. Wiśniewski, F. Z. Gaugaz, *Anal. Chem.* **2015**, *87*, 4110.
[21] E. A. K. Fletcher, M. Eltahir, F. Lindqvist, J. Rieth, G. Törnqvist, J. Leja-Jarblad, S. M. Mangsbo, *Int. Immunopharmacol.* **2018**, *54*, 1.
[22] R. R. French, H. T. C. Chan, A. L. Tutt, M. J. Glennie, *Nat. Med.* **1999**, *5*, 548.
[23] M. Eltahir, E. Fletcher, L. Dynesius, J. L. Jarblad, M. Lord, I. Laurén, M. Zekarias, X. Yu, M. S. Cragg, C. Hammarström, K. H. Levedahl, M. Höglund, G. Ullenhag, M. Mattsson, S. M. Mangsbo, *Int. Immunopharmacol.* **2021**, *90*, 107226.
[24] K. Nopora, C. A. Bernhard, C. Ried, A. A. Castello, K. M. Murphy, P. Marconi, U. Koszinowski, T. Brocker, *Front. Immunol.* **2012**, *3*, 348.
[25] E. M. Janssen, E. E. Lemmens, T. Wolfe, U. Christen, M. G. Von Herrath, S. P. Schoenberger, *Nature* **2003**, *421*, 852.
[26] A. L. White, H. T. C. Chan, R. R. French, J. Willoughby, C. I. Mockridge, A. Roghanian, C. A. Penfold, S. G. Booth, A. Dodhy, M. E. Polak, E. A. Potter, M. R. Ardern-Jones, J. S. Verbeek, P. W. M. Johnson, A. Al-Shamkhani, M. S. Cragg, S. A. Beers, M. J. Glennie, *Cancer Cell* **2015**, *27*, 138.
[27] M. Eltahir, H. Persson, S. Mangsbo, *Expert Opin. Biol. Ther.* **2020**, *20*, 215.
[28] X. Yu, H. T. C. Chan, C. M. Orr, O. Dadas, S. G. Booth, L. N. Dahal, C. A. Penfold, L. O'Brien, C. I. Mockridge, R. R. French, P. Duriez, L. R. Douglas, A. R. Pearson, M. S. Cragg, I. Tews, M. J. Glennie, A. L. White, *Cancer Cell* **2018**, *33*, 664.
[29] X. Yu, H. T. C. Chan, H. Fisher, C. A. Penfold, J. Kim, T. Inzhelevskaya, C. I. Mockridge, R. R. French, P. J. Duriez, L. R. Douglas, V. English, J. S. Verbeek, A. L. White, I. Tews, M. J. Glennie, M. S. Cragg, *Cancer Cell* **2020**, *37*, 850.
[30] G. J. D. Van Mierlo, A. T. Den Boer, J. P. Medema, E. I. H. Van Der Voort, M. F. Fransen, R. Offringa, C. J. M. Melief, R. E. M. Toes, *Proc. Natl. Acad. Sci. USA* **2002**, *99*, 5561.
[31] H. D. Lum, I. N. Buhtoiarov, B. E. Schmidt, G. Berke, D. M. Paulnock, P. M. Sondel, A. L. Rakhmilevich, *J. Leukocyte Biol.* **2006**, *79*, 1181.
[32] G. L. Beatty, E. G. Chiorean, M. P. Fishman, B. Saboury, U. R. Teitelbaum, W. Sun, R. D. Huhn, W. Song, D. Li, L. L. Sharp, D. A. Torigian, P. J. O'Dwyer, R. H. Vonderheide, *Science* **2011**, *331*, 1612.
[33] S. M. M. Irenaeus, D. Nielsen, P. Ellmark, J. Yachnin, A. Deronic, A. Nilsson, P. Norlén, N. Veitonmäki, C. S. Wennersten, G. J. Ullenhag, *Int. J. Cancer* **2019**, *145*, 1189.
[34] S. Ye, D. Cohen, N. A. Belmar, D. Choi, S. S. Tan, M. Sho, Y. Akamatsu, H. Kim, R. Iyer, J. Cabel, M. Lake, D. Song, J. Harlan, C. Zhang, Y. Fang, A. F. Wahl, P. Culp, D. Hollenbaugh, D. T. Chao, *Cancer Immunol. Res.* **2019**, *7*, 1864.
[35] J. J. Luke, L. Fong, K. Chung, A. W. Tolcher, K. Kelly, A. Hollebecque, C. Le Tourneau, V. Subbiah, F. Tsai, S. Kao, P. Cassier, M. Khasraw, K. Allaire, F. Fan, H. Fang, M. Patel, W. Henner, J. Hayflick, M. McDevitt, F. Barlesi, *Ann. Oncol.* **2019**, *30*, v498.
[36] L. Lu, N. Liu, K. Fan, G. Zhang, C. Li, Y. Yan, T. Liu, W. H. Fu, *Mol. Immunol.* **2019**, *109*, 149.
[37] P. Ellmark, K. Hägerbrand, M. Levin, L. Von Schantz, A. Deronic, L. Varas, A. Säll, K. Barchan, D. Werchau, L. Ljug, M. Thageson, A. Rosen, C. Sakellariou, M. Lindstedt, P. Ellmark, *J. Immunother. Cancer* **2020**, *8*, A911.
[38] T. So, M. Takenoyama, M. Mizukami, Y. Ichiki, M. Sugaya, T. Hanagiri, K. Sugio, K. Yasumoto, *Cancer Res.* **2005**, *65*, 5945.
[39] G. H. Nam, Y. Choi, G. B. Kim, S. Kim, S. A. Kim, I. S. Kim, *Adv. Mater.* **2020**, *32*, 2002440.
[40] K. Gabrusiewicz, X. Li, J. Wei, Y. Hashimoto, A. L. Marisetty, M. Ott, F. Wang, D. Hawke, J. Yu, L. M. Healy, A. Hossain, J. C. Akers, S. N. Maiti, S. Yamashita, Y. Shimizu, K. Dunner, M. A. Zal, J. K. Burks, J. Gumin, F. Nwajei, A. Rezavanian, S. Zhou, G. Rao, R. Sawaya, G. N. Fuller, J. T. Huse, J. P. Antel, S. Li, L. Cooper, E. P. Sulman, et al., *Oncoimmunology* **2018**, *7*, e1412909.
[41] F. Chalmin, S. Ladoire, G. Mignot, J. Vincent, M. Bruchard, J. P. Remy-Martin, W. Boireau, A. Rouleau, B. Simon, D. Lanneau, A. De Thonel, G. Multhoff, A. Hamman, F. Martin, B. Chauffert, E. Solary, L. Zitvogel, C. Garrido, B. Ryffel, C. Borg, L. Apetoh, C. Rébé, F. Ghiringhelli, *J. Clin. Invest.* **2010**, *120*, 457.
[42] R. A. Rosalia, E. D. Quakkelaar, A. Redeker, S. Khan, M. Camps, J. W. Drijfhout, A. L. Silva, W. Jiskoot, T. van Hall, P. A. van Veelen, G. Janssen, K. Franken, L. J. Cruz, A. Tromp, J. Oostendorp, S. H. van der Burg, F. Ossendorp, C. J. M. Melief, *Eur. J. Immunol.* **2013**, *43*, 2554.
[43] M. L. Disis, J. R. Gralow, H. Bernhard, S. L. Hand, W. D. Rubin, M. A. Cheever, *J. Immunol.* **1996**, *156*, 3151.
[44] E. M. J. van Brummelen, W. Ros, G. Wolbink, J. H. Beijnen, J. H. M. Schellens, *Oncologist* **2016**, *21*, 1260.
[45] K. P. Pratt, *Antibodies* **2018**, *7*, 19.
[46] A. K. Sato, M. Viswanathan, R. B. Kent, C. R. Wood, *Curr. Opin. Biotechnol.* **2006**, *17*, 638.
[47] R. Léger, K. Thibaudeau, M. Robitaille, O. Quraishi, P. van Wyk, N. Bousquet-Gagnon, J. Carette, J. P. Castaigne, D. P. Bridon, *Bioorg. Med. Chem. Lett.* **2004**, *14*, 4395.
[48] J. A. Dumont, S. C. Low, R. T. Peters, A. J. Bitonti, *BioDrugs* **2006**, *20*, 151.
[49] L. Bonifaz, D. Bonnyay, K. Mahnke, M. Rivera, M. C. Nussenzweig, R. M. Steinman, *J. Exp. Med.* **2002**, *196*, 1627.
[50] R. H. Vonderheide, *Annu. Rev. Med.* **2020**, *71*, 47.
[51] P. Johnson, R. Challis, F. Chowdhury, Y. Gao, M. Harvey, T. Geldart, P. Kerr, C. Chan, A. Smith, N. Steven, C. Edwards, M. Ashton-Key, E. Hodges, A. Tutt, C. Ottensmeier, M. Glennie, A. Williams, *Clin. Cancer Res.* **2015**, *21*, 1321.
[52] P. Bruhns, B. Iannascoli, P. England, D. A. Mancardi, N. Fernandez, S. Jorieux, M. Daëron, *Blood* **2009**, *113*, 3716.

© 2022 The Authors. Advanced Therapeutics published by Wiley-VCH GmbH